Time-lapsing biodiversity: an open source method for measuring diversity changes by remote sensing

Duccio Rocchini[1,2,3,4*], Matteo Marcantonio[5], Daniele Da Re[6], Gherardo Chirici[7], Marta Galluzzi[7], Jonathan Lenoir[8], Carlo Ricotta[9], Michele Torresani[10], Guy Ziv[11]

April 24, 2019

[1] University of Trento, Center Agriculture Food Environment (C3A), Via E. Mach 1, 38010 S. Michele all'Adige (TN), Italy

[2] University of Trento, Department of Cellular, Computational and Integrative Biology (CIBIO), Via Sommarive, 9, 38123 Povo (TN), Italy

[3] Fondazione Edmund Mach, Research and Innovation Centre, Department of Biodiversity and Molecular Ecology, Via E. Mach 1, 38010 S. Michele all'Adige (TN), Italy

[4] Czech University of Life Sciences Prague, Faculty of Environmental Sciences, Department of Applied Geoinformatics and Spatial Planning, Kamýcka 129, Praha - Suchdol, 16500, Czech Republic

[5] Department of Pathology, Microbiology, and Immunology, School of Veterinary Medicine, University of California, Davis, USA

[6] Earth and Life Institute, Université catholique de Louvain, Place Louis Pasteur 3, 1348, Louvain-la-Neuve, Belgium

[7] geoLAB - Laboratory of Forest Geomatics, Department of Agricultural, Food and Forestry Systems, University of Florence, Via San Bonaventura, 13, 50145 Firenze, Italy

[8] UR "Ecologie et dynamique des systèmes anthropisées" (EDYSAN, UMR 7058 CNRS-UPJV), Université de Picardie Jules Verne, 1 Rue des Louvels, 80037 Amiens Cedex 1, France

[9] Department of Environmental Biology, University of Rome "La Sapienza", Rome 00185, Italy

[10] Free University of Bolzano/Bozen, Faculty of Science and Technology, Piazza Universitá / Universitätsplatz 1, 39100, Bolzano/Bozen, Italy

[11] School of Geography, University of Leeds, Leeds LS2 9JT, UK

* corresponding author: duccio.rocchini@unitn.it

Abstract

Understanding biodiversity changes in time is crucial to promptly provide management practices against diversity loss. This is overall true when considering global scales, since human-induced global change is expected to make significant changes on the Earth's biota. Biodiversity management and planning is mainly based on field observations related to community diversity, considering different taxa. However, such methods are time and cost demanding and does not allow in most cases to get temporal replicates. In this view, remote sensing can provide for a wide data coverage in a short period of time. Recently, the use of Rao's Q diversity as a measure of spectral diversity has been proposed in order to explicitly taking into account differences in a neighborhood considering abundance and relative distance among pixels. The aim of this paper was to extend such a measure over the temporal dimension and to present an innovative approach to calculate remotely sensed temporal diversity. We demonstrated that temporal beta-diversity (spectral turnover) can be calculated pixel-wise in terms of both slope and coefficient of variation and further plotted over the whole matrix / image. From an ecological and operational point of view, for prioritisation practices in biodiversity protection, temporal variability could be beneficial in order to plan more efficient conservation practices starting from spectral diversity hotspots in space and time. In this paper we delivered a highly reproducible approach to calculate spatio-temporal diversity in a robust and straightforward manner. Since it is based on open source code, we expect that our method will be further used by several researchers and landscape managers.

keywords: biodiversity; ecological informatics; Rao's Q diversity; remote sensing; satellite imagery; temporal variability

1 Introduction

Understanding biodiversity changes in time is crucial to promptly provide management practices against diversity loss (Gaston, 2008).

This has been proven for various part of the globe, considering different biomes and habitat types like dry (Nagendra et al., 2010) and humid (Somers et al., 2015) tropical forests, savannas (Oldeland et al., 2010), grasslands (Feilhauer et al., 2013), among the others.

This is overall true when considering global scales, since human-induced global change is expected to make significant changes on the Earth's biota (Moreno et al., 2017). This is explicitly taken into account by the Sustainable Development Goals of the United Nations (`https://www.un.org/sustainabledevelopment/sustainable-development-goals/`), with Goal 15 explicitly aiming to "halt biodiversity loss".

However, biodiversity management and planning is mainly based on field observations related to community diversity, considering different taxa, under the assumption of robust statistical sampling and proper methods of analysis (e.g. Chiarucci et al. (2017)). Such a method is time and cost consuming and does not allow in most cases to get temporal replicates.

This led to the urgent need of developing worldwide research and stakeholders networks to face climate and biodiversity change at global scale, like the Global Climate Observing System (GCOS, `https://public.wmo.int/`), the Intergovernmental Panel on Climate Change (IPCC, `http://www.ipcc.ch/`) or the Group on Earth Observations - Biodiversity Observation Network (GEO BON, https://geobon.org/). Essential Climate Variables (ECVs) and the Essential Biodiversity Variables (EBVs, see Pereira et al. (2013)) were thus the main outputs of such networks, as proxies of Earth global change in space and time.

In this framework, remote sensing has been proposed as a straightforward operational tool providing a wide data coverage in a short period of time (Rocchini and Di Rita, A. , 2005; Skidmore et al., 2015), helping to save costs and time. Furthermore, measures of diversity from remotely sensed vs. field data showed a positive relationship, leading to consider remote sensing diversity as a direct proxy of the variation of biodiversity in space (Gillespie et al., 2008; Lausch et al., 2016).

Most of the remote sensing-based measures of spectral diversity have been widely based on i) the spatial variability of pixel values by measuring pairwise distances in a spectral space (Feret and Asnaer, 2014; Somers et al., 2015) or on ii) measures of relative abundance of values based on information theory (Ricotta, 2005).

Recently, Rocchini et al. (2017) proposed the use of Rao's Q diversity as a measure of spectral diversity which explicitly takes into account differences in a neighbourhood relying on abundance and relative distance among pixels, extending for the first time to 2D-matrices (satellite images) the measure firstly proposed by Rao (1982).

This might allow the so called continuous field mapping which in most cases has been applied to land cover classification (Mathys et al., 2009) but it is also a valuable tool for diversity mapping over wide geographical regions, mainly based on moving window methods. Basically, starting from the spectral mixing space of a satellite image, one can measure the continuous variability of pixel values in space by local-based measures, which maximise the contrast in spectral diversity highlighting hotspots of diversity, mainly related to transition zones in space (Small, 2005).

The temporal dimension, coupled with spatial approaches, might help inferring biodiversity change over large areas. While this has been widely acknowledged in some ecological modelling practices, like in environmental niche modelling (Feng and Papes, 2017), it has rarely been explicitly considered when dealing with remotely sensed diversity measurements, over wider temporal scales. In this view, most of the research efforts have been devoted to phenology (He et al., 2009) without an explicit spatial approach to measure spectral turnover in space and time.

The aim of this paper is to present an innovative approach to calculate the temporal change of remotely sensed diversity. We will first introduce the theoretical background of the diversity calculation in time and then provide an empirical example based on MODIS data, by also providing the complete R code (Appendix 1 or `https://gitlab.com/danidr/temporal_rs_biodiversity/blob/master/RocchiniEtAl_2019_slopes.R`).

2 Benchmark example

2.1 Algorithm development

Rao's Q diversity explicitly considers both relative abundance and spectral distances among pixel reflectance values as:

$$Q = \sum \sum d_{ij} \times p_i \times p_j \tag{1}$$

where d_{ij} = pairwise distance between pixels attaining to reflectance values i and j, p_i = relative abundance of pixels attaining to reflectance value i, and p_j = relative abundance of pixels attaining to reflectance value j. As proposed by Rocchini et al. (2017), given an input 2D matrix (image)

$$I = \begin{pmatrix} P_{1,1} & P_{1,2} & P_{1,3} & \dots & P_{1,n} \\ P_{2,1} & P_{2,2} & P_{2,3} & \dots & P_{2,n} \\ \vdots & \vdots & \vdots & \ddots & \vdots \\ P_{m,1} & P_{m,2} & P_{m,3} & \dots & P_{m,n} \end{pmatrix} \tag{2}$$

where P=input pixel, Rao's Q can be calculated by a moving window (spatial kernel or 2D matrix)

$$M = \begin{pmatrix} P_{1,1} & P_{1,2} & P_{1,3} \\ P_{2,1} & P_{2,2} & P_{2,3} \\ P_{3,1} & P_{3,2} & P_{3,3} \end{pmatrix} \tag{3}$$

using $n \times n$ pixels in a neighbourhood of a given site (pixel) by returning an output map of local alpha-diversity hotspots.

Rao's Q diversity value applied to remotely sensed images allows one to discriminate among environmental situations with low or high evenness, as the mostly used Shannon's H' does, but also including distance among pixel vaues. Given an image I, Figure 1 shows four different situations, starting from the lowest diversity in the environment (Figure 1A), with pixels which are similar to each other (low distance) and with one value dominating the landscape (low evenness). On the contrary, Figure 1D represents the highest possible diversity with a high distance among pixels and a high evenness (equidistribution of pixel values). While information theory based on Shannon's H' allows discriminating between extreme situations, it does not allow discriminating diversity hotspots deriving from i) a high evenness of pixel values but with a low distance among them (similar environments) and ii) a high evenness of pixel values with a high distance among them (very different environments). Since in environmental science and in remote sensing of environmental diversity the interest is pointed to the detection of strong differences among environment, i.e. diversity hotpots, the Rao's Q diversity seems to perform better with respect to common information theory based calculus. The mathematical calculation of Shannon's H' and Rao's Q values is provided in Appendix 2, which is performed by the algorithm described in Rocchini et al. (2017) and freely available under the GitHub flagship project at: `https://github.com/mattmar/spectralrao/blob/master/spectralrao.r`.

In general, the output Rao's Q diversity map is derived at a certain time t_0, based on the date of the original input image being used. In this paper we are aiming at summarizing different output maps derived in different times as:

$$O_{t0} = \begin{pmatrix} P_{1,1}t0 & P_{1,2}t0 & P_{1,3}t0 & \dots & P_{1,n}t0 \\ P_{2,1}t0 & P_{2,2}t0 & P_{2,3}t0 & \dots & P_{2,n}t0 \\ \vdots & \vdots & \vdots & \ddots & \vdots \\ P_{m,1}t0 & P_{m,2}t0 & P_{m,3}t0 & \dots & P_{m,n}t0 \end{pmatrix} \tag{4}$$

$$O_{t1} = \begin{pmatrix} P_{1,1}t1 & P_{1,2}t1 & P_{1,3}t1 & \dots & P_{1,n}t1 \\ P_{2,1}t1 & P_{2,2}t1 & P_{2,3}t1 & \dots & P_{2,n}t1 \\ \vdots & \vdots & \vdots & \ddots & \vdots \\ P_{m,1}t1 & P_{m,2}t1 & P_{m,3}t1 & \dots & P_{m,n}t1 \end{pmatrix} \tag{5}$$

$$O_{tn} = \begin{pmatrix} P_{1,1}tn & P_{1,2}tn & P_{1,3}tn & \dots & P_{1,n}tn \\ P_{2,1}tn & P_{2,2}tn & P_{2,3}tn & \dots & P_{2,n}tn \\ \vdots & \vdots & \vdots & \ddots & \vdots \\ P_{m,1}tn & P_{m,2}tn & P_{m,3}tn & \dots & P_{m,n}tn \end{pmatrix} \tag{6}$$

In other words, the present manuscript seeks to find a method to account for the change in time of Rao's Q diversity.

Let $\mathrm{Q}_{P_0 t_0}$ be the Rao's Q value at a given site (pixel P_0) in a certain moment (time t_0, Figure 2). The $\mathrm{Q}_{P_0 t_x}$ value can be viewed in a linear time space from t_0 to t_n. Once such values have been plotted, a locally weighted scatter-plot smoothing (LOWESS) function, also referred to as LOESS (Cleveland

, 1979; Cleveland and Devlin, 1988), can be estimated, which reduces to a linear function $y \sim x$ in case of linear variability. LOESS fits a function to a subset of the data, generally splitting the explanatory variable and giving a higher weight to points near the point where the response is being estimated.

The mean slope (trend) of the LOESS is expected to represent the change of Rao's Q diversity in time. In order to get a pixel-wise approximation of the slope we extracted the derivative of the Rao's Q diversity smoothed temporal function at each t_i, computing the $\triangle$y/$\triangle$x. Then, the descriptive statistics over the whole time series were calculated, giving information on the smoothed function trend.

As a proxy of the variation of the Rao's Q diversity values over the whole time series, a temporal coefficient of variation index (CV) was computed following Hijmans (2004). This index, expressed as a percentage, is the ratio between the standard deviation and the mean of all the Rao's Q diversity values. Larger percentages represent a higher spectral-turnover, providing a beta-diversity quantification.

Summarising, the average slope of the LOESS curve is expected to represent the amount of mean diversity along a temporal trend, while its coefficient of variation would represent the temporal turnover in the spectral Rao's Q. Temporal diversity can thus be calculated pixel-wise in terms of both slope and coefficient of variation and further plotted over the whole matrix / image.

In order to implement an empirical example of the method being proposed, we made use of the free set of Rao's Q data based on MODIS NDVI images at a resolution of 5km provided in Rocchini et al. (2018). A sketch of the original MODIS NDVI input set is provided in Appendix 3. In order to rely on a high complexity landscape we decided to focus on the italian peninsula, which guarantees a high ecological gradient from the sea to high mountain alps (until 4000 metres). Based on the open source code provided in Appendix 1, the method can be straightfowardly extended to other areas, habitats, or biomes. The final stack of layers consisted of 17 Rao's Q images gathered from 2000 to 2016 in June (Figure 3).

Each pixel was projected in a temporal space according to Figure 2 from 2000 to 2016, and a LOESS function with automatic smoothing parameter selection through bias-corrected Akaike information criterion (AICc) was fitted relying on the r package `fANCOVA` (Wang, 2010), building a global set of N functions where N = number of pixels in the image. The mean slope and the coefficient of variation along the temporal gradient of the LOESS function was calculated for each pixel and further spatially plotted.

2.2 Results

Rao's Q temporal diversity considering LOESS mean slope (mean temporal diversity) and LOESS coefficient of variation (temporal turnover) showed a discriminant pattern among different areas (Figure 4). Both measures detected a higher temporal diversity in areas with higher landscape morphological complexity detected by the spatial Rao's Q (see Figure 3) with an enhancement in the relative temporal beta-diversity (turnover) detected by the coefficient of variation of the LOESS function.

Spatial Rao's Q showed a high value in Italy in topographically and ecologically complex mountain areas, including Alps and Appennines (central italy) (Figure 3). However, once considering the temporal dimension, alpine areas showed a higher relative value of Rao's Q temporal variation, considering both mean and turnover in temporal diversity (Figure 4). This pattern has also been hypothesized, but never specifically tested until now, by Rocchini et al. (2011) who stressed the possibility of a higher variation in space and time of top mountainous areas (in particular, Alps) which are expected to show a high amount of ecologically contrasting traits, from agricultural areas to conifers and broadleaf forests, to pastures, grasslands and bare rocks (Pelorosso et al., 2011).

3 Discussion

Estimating values of diversity over an area given a sample is crucial for a number of different ecological tasks (Granger et al., 2015). Remote sensing certainly represents a powerful tool for getting estimated diversity values in a 2D surface. Extending on Ricotta (2008), who calculated community beta-diversity starting from species presence / absence scores, in this paper we propose to substitute such scores with pixel based values, being such values diversity measures (like the Rao's Q scores) or original reflectances in a satellite image, by further redistributing them in a new time-system to carry out a LOESS based calculation of diversity changes.

In this view, the variability of diversity over space has been investigated at different spatial scales and with different approaches (refer to Rocchini et al. (2010) for a review). As stressed by Leitao et al. (2015), it might be crucial to find methods readily available to deal with time series data, in order to potentially account for the time axis in the analysis of beta-diversity change.

Our method represents a powerful approach to estimate remotely sensed beta-diversity in time, at large spatial extents. Once coupled with hierarchical methods to also account for different scales of diversities, e.g. with Bayesian hierarchical modelling (Zhang et al., 2014), our approach might represent a benchmark for modelling the variability in space and time of diversity at multiple spatial scales. It is far beyond the aim of this paper to test the sensitivity of the method to different spatial grains and spectral resolutions, but since it is based on pixel distances and relative abundance we expect that it can be applied to any kind of multi- or hyper-volumes like multi- or hyper-spectral images at different spatial and spectral resolutions from high (e.g. Quickbird, Ikonos) to medium (e.g. Sentinel-2 or Landsat data) and low grains (like MODIS data in our case).

Furthermore, our method might help measuring not only spatial variations in beta-diversity to be related directly to the effect of ecosystem dynamics (Wang and Loreau, 2014), but also supply a synthesis of temporal variations in beta-diversity thus implicitly incorporating such dynamcis.

In some cases, spatial non-stationarity has been advocated as one of the major problems when the variability of a certain variable is non-uniform in space (Osborne et al., 2007). In our case, we would promote our approach to also account for potential anomalies, or simply spots of diversity variation in time, when measuring beta-diversity from satellites. As an example, Mathys et al. (2009) proved that, when dealing with land cover continuous variability over space, adding spectral diversity derived from remotely sensed images could improve modelling performance.

There are intrinsic difficulties related to the estimate of biodiversity changes in time (temporal beta-diversity) mainly related to the sampling replication in the same location with the same sampling protocol. Permanent plots arranged in networks like the Long Term Ecosystem Research in Europe (LTER, http://www.lter-europe.net/) have been explicitly implemented to solve the problem. However, they represent sporadic and spatially scattered locations in local areas. Once zones with high spatial and temporal variability have been detected, the attained information could be a powerful tool for guiding field based surveys of species diversity (Rocchini et al., 2005). This is overall true when considering ancillary models specifically dedicated to the development of efficient sampling designs, based on e.g. sampling optimisation based on synthetic maps (Schweiger et al., 2015) or on virtual species sets (Garzon-Lopez et al., 2016).

Landscape metrics (e.g., patch area and connectivity) have been widely used as tools for identification of areas with higher biodiversity, but they mostly refers to categorical maps such as land cover (Katayama et al., 2014; Morelli et al., 2018). However, land cover maps are generally an oversimplification of habitat variability Amici et al. (2017) and should be used with care to avoid the underestimation of the continuous ecological variability over the landscape (Austin , 1987; Palmer et al., 2002; Rocchini, 2007).

In this paper, the continuous variability of spectral pixel values, coupled with the temporal dimension provided for additional information on the variation of ecosystems, allowing a better detection of highly diverse spot in space and in time, considering different time spans t0, t1, ..., tn. Strictly speaking, including temporal variation in the analysis of diversity from remote sensing might provide additional information to spatial kernels measured at t0.

Obviously, the variability of the spectral signal is not the only proxy of diversity, and in some cases (e.g. in urban areas) a high environmental variability is not necessarily related to a high amount of biodiversity in the field (Ricotta et al., 2010). However, in case of natural and seminatural areas, spectral variability might represent one of the main proxies of diversity (Skidmore et al., 2015; Schmeller et al., 2017). Hence, in order to measure spatial and temporal changes in diversity, it could be coupled with additional variables such as: i) climatic predictors (Zellweger et al., 2019), ii) soil properties (Tuomisto et al., 2003), iii) topographical complexity (Badgley et al., 2017). Furthermore, in this manuscript we made use of a spectral index like the inter-annual NDVI as an example dataset to calculate spatial heterogeneity, as in Oindo and Skidmore (2002) or Gillespie (2005) and more recently Feilhauer et al. (2012), by deriving the Rao's Q diversity on a continuous data matrix to monitor heterogeneity changes through time, although the annual inter-variation of productivity could be related to several factors, and not just to niche-based diversity changes. We refer to the debate between Krishnaswamy et al. (2009) and Rocchini (2009) about problems related to alpha- and beta-diversity measurement from NDVI.

4 Conclusion

In this paper we presented a robust and reproducible approach to estimate the temporal ecosystems' beta-diversity based on a locally weighted scatterplot smoothing. We applied it to the spatial Rao's Q diversity proposed by Rocchini et al. (2017), but the method could be ported to any spatial diversity measure made in a spectral space.

Being based on open source coding, we expect a high reproducibility of the proposed approach, and stimulate researchers to test it in different habitats, by varying spatial grains and extents and potentially making use of different sensors.

The open source code provided will guarantee the robustness and reproducibility of the method. In fact, we are expecting that such a code will be used by other researchers to further develop additional algorithms on temporal variability measurement from satellite images.

From an ecological and operational point of view, for species inventorying maximisation in biodiversity protection, advocated by the Sustainable Development Goal 15 ("halt biodiversity loss") and scientifically proposed by Rocchini et al. (2005) and more recently reviewed by Schmeller et al. (2017), the temporal variability, together with the spatial one, could be beneficial in order to plan more efficient conservation practices starting with those diversity hotspots detected in space and time by remote sensing techniques.

Attempts have been made to measure the spatial sensitivity of the relation between species and spectral diversity (Wang et al., 2018) which might impact further management practices if disregarded. However, as far as we know, nothing has been done to project it also in time. Our method represents a potential benchmark for applying such a variation measurement in time, which could be extended i) not only to other types of sensors in satellite images but to every kind of 2D matrices including species-plot arrays, ii) to other methods such as the measure of spatial and temporal autocorrelation (Guelat and Kery, 2008), iii) to additional ecospaces (sensu Dick and Laflamme (2018)) by fuzzy modelling.

5 Acknowledgements

Computational resources have been provided by the supercomputing facilities of the Université catholique de Louvain (CISM/UCL) and the Consortium des Equipements de Calcul Intensif en Fédération Wallonie Bruxelles (CECI) funded by the Fond de la Recherche Scientifique de Belgique (FRS-FNRS).

We thank two anonymous reviewers who provided useful insights on a previous version of this manuscript.

DR was supported by the H2020 project ECOPOTENTIAL (grant agreement 641762) and the H2020 TRuStEE - Training on Remote Sensing for Ecosystem Modelling project (grant agreement 721995).

References

Amici, V., Marcantonio, M., La Porta, N., Rocchini, D.(2017). A multi-temporal approach in Max-Ent modelling: A new frontier for land use/land cover change detection. Ecological Informatics, 40: 40-49.

Austin, M.P. (1987). Models for the analysis of species' response to environmental gradients. Vegetatio, 69: 35-45.

Badgley, C., Smiley, T.M., Terry, R., Davis, E.B., DeSantis, L.R.G., Fox, D.L., Hopkins, S.S.B., Jezkova, T., Matocq, M.D., Matzke, N., McGuire, J.L., Mulch, A., Riddle, B.R., Roth, V.L., Samuels, J.X., StrÃűmberg, C.A.E., Yanites, B.J. (2017). Biodiversity and topographic complexity: modern and geohistorical perspectives. Trends in Ecology & Evolution, 32: 211-226.

Chiarucci, A., Bacaro, G., Rocchini, D., Ricotta, C., Palmer, M.W., Scheiner, S.M. (2009). Spatially constrained rarefaction: incorporating the autocorrelated structure of biological communities in sample-based rarefaction. Community Ecology, 10: 209-214.

Cleveland, W.S. (1979) Robust locally weighted regression and smoothing scatterplots. Journal of the American Statistical Association, 74: 829-836.

Cleveland, W.S., Devlin, S.J. (1988). Locally weighted regression: an approach to regression analysis by local fitting. Journal of the American Statistical Association, 83: 596-610.

Dick, D.G., Laflamme, M. (2018). Fuzzy Ecospace Modelling. Methods in Ecology and Evolution. Accepted. doi:10.1111/2041-210X.13010

Ewald, M., Aerts, R., Lenoir, J., Fassnacht, F.E., Nicolas, M., Skowronek, S., Piat, J., Honnay, O., Garzon-Lopez, C.-X., Feilhauer, H., Van De Kerchove, R., Somers, B., Hattab, T., Rocchini, D., Schmidtlein, S. (2018). LiDAR derived forest structure data improves predictions of canopy N and P concentrations from imaging spectroscopy. Remote Sensing of Environment, 211: 13-25.

Feilhauer, H., He, K.S., Rocchini, D. (2012). Modeling species distribution using niche-based proxies derived from composite bioclimatic variables and MODIS NDVI. Remote Sensing, 4: 2057-2075.

Feilhauer, H., Thonfeld, F., Faude, U., He, K.S., Rocchini, D., Schmidtlein, S. (2013). Assessing floristic composition with multispectral sensors - A comparison based on monotemporal and multiseasonal field spectra. International Journal of Applied Earth Observation and Geoinformation, 21: 218-229.

Feng, X., Papes, M. (2017). Physiological limits in an ecological niche modeling framework: A case study of water temperature and salinity constraints of freshwater bivalves invasive in USA. Ecological Modelling, 346: 48-57.

Feret, J.-B., Asner, G.P. (2014). Mapping tropical forest canopy diversity using high-fidelity imaging spectroscopy. Ecological Applications, 24: 1289-1296.

Garzon-Lopez, C.X., Bastin, L., Foody, G.M., Rocchini, D. (2016). A virtual species set for robust and reproducible Species Distribution Modelling tests. Data in Brief, 7: 476-479.

Gaston, K.J. (2008). Biodiversity and extinction: the dynamics of geographic range size. Progress in Physical Geography, 32: 678-683.

Gillespie, T.W. (2005). Predicting woody-plant species richness in tropical dry forests: a case study from South Florida, USA. Ecological Applications, 15: 27-37.

Gillespie, T.W., Foody, G.M., Rocchini, D., Giorgi, A.P., Saatchi, S. (2008). Measuring and modelling biodiversity from space. Progress in Physical Geography, 32: 203-221.

Granger, V. , Bez, N. , Fromentin, J. , Meynard, C. , Jadaud, A. , MÃľrigot, B., PeresâĂŘNeto, P. (2015), Mapping diversity indices: not a trivial issue. Methods in Ecology and Evolution, 6: 688-696.

Guelat, J., Kery, M. (2018). Effects of spatial autocorrelation and imperfect detection on species distribution models. Methods in Ecology and Evolution. Accepted. doi:10.1111/2041-210X.12983

He, K.S., Zhang, J., Zhang, Q. (2009). Linking variability in species composition and MODIS on beta diversity measurements. Acta Oecologica, 35: 14-21.

Hijmans, R.J. (2004). Arc Macro Language (AML) version 2.1 for calculating 19 bioclimatic predictors: Berkeley, Calif, Museum of Vertebrate Zoology, University of California at Berkeley. Available at http://www.worldclim.org/bioclim.

Katayama, N., Amano, T., Naoe, S., Yamakita, T., Komatsu, I., Takagawa, S., Sato, N., Ueta, M., Miyashita, T. (2014). Landscape heterogeneity-biodiversity relationship: effect of range size. PLoS ONE, 9: e93359.

Krishnaswamy, J., Bawa, K.S., Ganeshaiah, K.N., Kiran, M.C. (2009). Quantifying and mapping biodiversity and ecosystem services: Utility of a multi-season NDVI based Mahalanobis distance surrogate. Remote Sensing of Environment, 113, 857-867.

Lausch, A., Bannehr, L., Beckmann, M., Boehm, C., Feilhauer, H., Hacker, J.M., Heurich, M., Jung, A., Klenke, R., Neumann, C., Pause, M., Rocchini, D., Schaepman, M.E., Schmidtlein, S., Schulz, K., Selsam, P., Settele, J., Skidmore, A.K., Cord, A.F. (2016). Linking Earth Observation and taxonomic, structural and functional biodiversity: Local to ecosystem perspectives. Ecological Indicators, 70: 317-339.

Leitao, P., Schwieder, M., Suess, S., Catry, I., Milton, E.J., Moreira, F., Osborne, P.E., Pinto, M.J., van der Linden, S., Hostert, P. (2015). Mapping beta diversity from space: Sparse Generalised Dissimilarity Modelling (SGDM) for analysing high-dimensional data. Methods in Ecology and Evolution, 6: 764-771.

Mathys, L., Guisan, A., Kellenberger, T.W., Zimmermann, N.E. (2009). Evaluating effects of spectral training data distribution on continuous field mapping performance. ISPRS Journal of Photogrammetry and Remote Sensing, 64: 665-673.

Morelli, F., Benedetti, Y., Simova, P. (2018).Landscape metrics as indicators of avian diversity and community measures. Ecological Indicators, 90: 132-141.

Moreno, C.E., Calderon-Patron, J.M., Arroyo-Rodriguez, V., Barragan, F., Escobar, F., GÃşmez-Ortiz, Y., MartÃŋn-Regalado, N., Martinez-Falcon, A.P., MartÃŋnez-Morales, M.A., Mendoza, E., Ortega-Martinez, I.J., Perez-Hernandez, C.X., Pineda, E., Pineda-Lopez, R., Rios-DÃŋaz, C.L., Rodriguez, P., Rosas, F., Schondube, J.E., Zuria, I. (2018). Measuring biodiversity in the Anthropocene: a simple guide to helpful methods. Biodiversity and Conservation, 26: 2993-2998.

Nagendra, H., Rocchini, D., Ghate, R., Sharma, B., Pareeth, S. (2010). Assessing plant diversity in a dry tropical forest: comparing the utility of Landsat and IKONOS satellite images. Remote Sensing, 2: 478-496.

Oindo, B.O., Skidmore, A.K. (2002). Interannual variability of NDVI and species richness in Kenya. International Journal of Remote Sensing 23: 285-298.

Oldeland, J., Wesuls, D., Rocchini, D., Schmidt, M., Norbert, J. (2010).

Does using species abundance data improve estimates of species diversity from remotely sensed spectral heterogeneity? Ecological Indicators, 10: 390-396.

Osborne, P.E., Foody, G.M., Suarez-Seoane, S. (2007). Non-stationarity and local approaches to modeling the distributions of wildlife. Diversity and Distributions, 13, 313-323.

Palmer, M.W., Earls, P.G., Hoagland, B.W., White, P.S., Wohlgemuth, T. (2002). Quantitative tools for perfecting species lists. Environmetrics, 13: 121-137.

Pereira, H.M., Ferrier, S., Walters, M., Geller, G., Jongman, R., Scholes, R., Bruford, M., Brummitt, N., Butchart, S., Cardoso, A. (2013). Essential biodiversity variables. Science, 339: 277-278.

Pelorosso, R., Della Chiesa, S., Tappeiner, U., Leone, A., Rocchini, D. (2011). Stability analysis for defining management strategies in abandoned mountain landscapes of the Mediterranean basin. Landscape and Urban Planning, 103: 335-346.

Rao, C.R. (1982). Diversity and dissimilarity coefficients: a unified approach. Theoretical Population Biology, 21: 24-43.

Ricotta, C. (2005). On possible measures for evaluating the degree of uncertainty of fuzzy thematic maps. International Journal of Remote Sensing, 26: 5573-5583.

Ricotta, C. (2008). Computing additive beta-diversity from presence and absence scores: A critique and alternative parameters. Theoretical Population Biology, 73: 244-249.

Ricotta, C., Godefroid, S., Rocchini, D. (2010). Patterns of native and exotic species richness in the urban flora of Brussels: rejecting the 'rich get richer' model. Biological Invasions, 12. 233-240.

Rocchini, D. (2009). Commentary on Krishnaswamy et al. - Quantifying and mapping biodiversity and ecosystem services: Utility of a multi-season NDVI based Mahalanobis distance surrogate. Remote Sensing of Environment, 113: 904-906.

Rocchini, D. (2007). Effects of spatial and spectral resolution in estimating ecosystem alpha-diversity by satellite imagery. Remote Sensing of Environment, 111: 423-434.

Rocchini, D., Andreini Butini, S., Chiarucci, A. (2005). Maximizing plant species inventory efficiency by means of remotely sensed spectral distances. Global Ecology and Biogeography, 14: 431-437.

Rocchini, D., Bacaro, G., Chirici, G., Da Re, D., Feilhauer, H., Foody, G.M., Galluzzi, M., Garzon-Lopez, C.X., Gillespie, T.W., He, K.S., Lenoir, J., Marcantonio, M., Nagendra, H., Ricotta, C., Rommel, E., Schmidtlein, S., Skidmore, A.K., Van De Kerchove, R., Wegmann, M., Rugani, B. (2018). Remotely sensed spatial heterogeneity as an exploratory tool for taxonomic and functional diversity study. Ecological Indicators, 85: 983-990.

Rocchini, D., Balkenhol, N., Carter, G.A., Foody, G.M. Gillespie, T.W., He, K.S., Kark, S., Levin, N., Lucas, K., Luoto, M., Nagendra, H., Oldeland, J., Ricotta, C., Southworth, J., Neteler, M. (2010). Remotely sensed spectral heterogeneity as a proxy of species diversity: recent advances and open challenges. Ecological Informatics, 5: 318-329.

Rocchini, D., Di Rita, A. (2005). Relief effects on aerial photos geometric correction. Applied Geography, 25: 159-168.

Rocchini, D., Hernandez Stefanoni, J.L., He, K.S: (2015). Advancing species diversity estimate by remotely sensed proxies: a conceptual review. Ecological Informatics, 25: 22-28.

Rocchini, D., Marcantonio, M., Ricotta, C. (2017). Measuring Rao's Q diversity index from remote sensing: an open source solution. Ecological Indicators, 72: 234-238.

Rocchini, D., McGlinn, D., Ricotta, C., Neteler, M., Wohlgemuth, T. (2011).

Landscape complexity and spatial scale influence the relationship between remotely sensed spectral diversity and survey-based plant species richness. Journal of Vegetation Science, 22: 688-698.

Schmeller, D., Weatherdon, L., Loyau, A., Bondeau, A., Brotons, L., Brummitt, N., Geijzendorffer, I., Haase, P., Kuemmerlen, M., Martin, C., Mihoub, J.-B., Rocchini, D., Saarenmaa, H., Stoll, S., Regan, E. (2017). A suite of essential biodiversity variables for detecting critical biodiversity change. Biological Reviews, 93: 55-71.

Schweiger, A.H., Irl, S.D.H., Steinbauer, M.J., Dengler, J., Beierkuhnlein, C. (2015). Optimizing sampling approaches along ecological gradients. Methods in Ecology and Evolution, 7: 463-471.

Skidmore, A.K., Pettorelli, N., Coops, N.C., Geller, G.N., Hansen, M., Lucas, R., Mucher, C.A., O'Connor, B., Paganini, M., Pereira, H.M., Schaepman, M.E., Wurner, W., Wang, T., Wegmann, M. (2015). Environmental science: agree on biodiversity metrics to track from space. Nature, 523: 403-405.

Small, C. (2005). A global analysis of urban reflectance. International Journal of Remote Sensing, 26: 661-681.

Somers, B., Asner, G.P., Martin, R.E., Anderson, C.B., Knapp, D.E., Wright, S.J., Van De Kerchove, R. (2015). Mesoscale assessment of changes in tropical tree species richness across a bioclimatic gradient in Panama using airborne imaging spectroscopy. Remote Sensing of Environment, 167: 111-120.

Tuomisto, H., Ruokolainen, K., Yli-Halla, M. (2003) Dispersal, environment, and floristic variation of western amazonian forests. Science, 299: 241-244.

Wang, X.-F. (2010). fANCOVA: Nonparametric Analysis of Covariance. R package version 0.5-1. https://CRAN.R-project.org/package=fANCOVA

Wang, S., Loreau, M. (2014). Ecosystem stability in space: alpha, beta and gamma variability. Ecology Letters, 17: 891-901.

Wang, R., Gamon, J.A., Cavender-Bares, J., Townsend, P.A., Zygielbaum, A.I. (2018). The spatial sensitivity of the spectral diversity-biodiversity relationship: an experimental test in a prairie grassland. Ecological Applications, 28: 541-556.

Zellweger, F., De Frenne, P., Lenoir, J., Rocchini, D., Coomes, D. (2019). Advances in microclimate ecology arising from remote sensing. Trends in Ecology & Evolution, 34: 327-341.

Zhang, J., Crist, T.O., Hou, P. (2014). Partitioning of alpha and beta diversity using hierarchical Bayesian modeling of species distribution and abundance. Environmental and Ecological Statistics, 21: 611-625.

$$
I = \begin{cases}
\begin{pmatrix} 100 & 100 & 100 \\ 100 & 100 & 100 \\ 101 & 101 & 101 \end{pmatrix} & \text{Low } E \text{ Low } D \\
\begin{pmatrix} 100 & 101 & 102 \\ 103 & 104 & 105 \\ 106 & 107 & 108 \end{pmatrix} & \text{High } E \text{ Low } D \\
\begin{pmatrix} 1 & 1 & 1 \\ 1 & 1 & 1 \\ 101 & 101 & 101 \end{pmatrix} & \text{Low } E \text{ High } D \\
\begin{pmatrix} 1 & 7 & 10 \\ 100 & 102 & 150 \\ 200 & 220 & 255 \end{pmatrix} & \text{High } E \text{ High } D
\end{cases}
$$

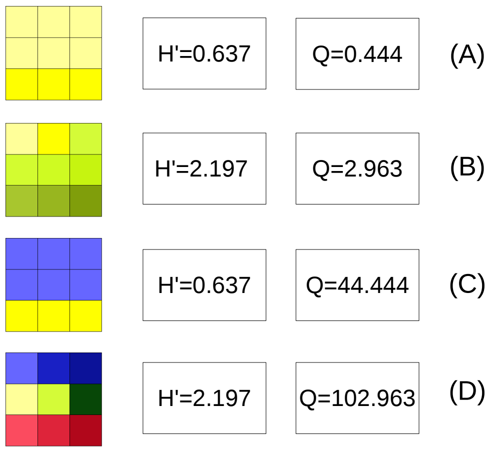

Figure 1: Synthetic example showing four different environmental situations and their relative Shannon's H' and Rao's Q indices. (A) Lower diversity in terms of both evenness and distance among pixel values; (B) and (C) intermediate situations; (D) higher diversity in terms of both evenness and distance among pixel values. Refer to the main text for additional information and to Appendix 2 for the mathematical calculation.

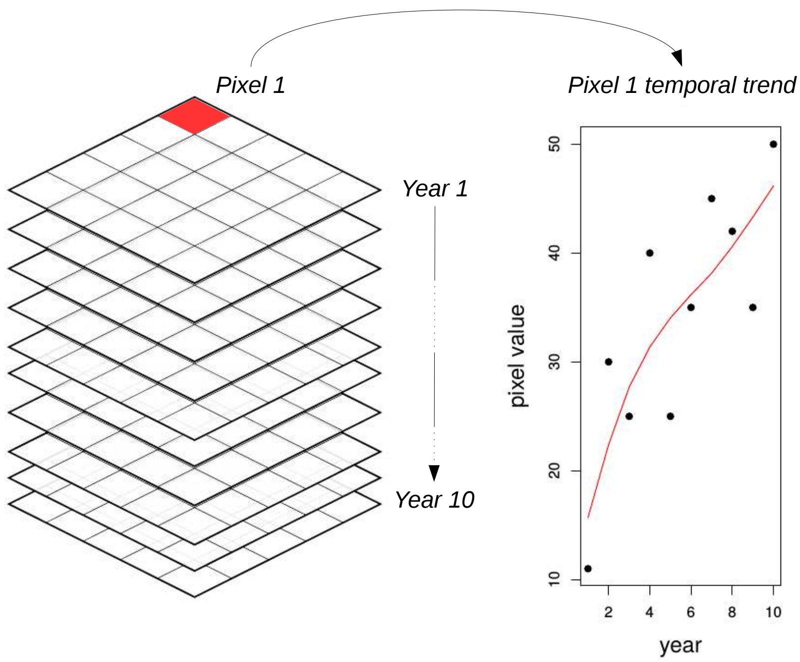

Figure 2: The Rao's value $Q_{P_0t_0}$ at a given site (pixel P_0) in a certain moment (time t_0) can be plotted on a time scale. Once all the values from $Q_{P_0t_0}$ to $Q_{P_0t_n}$ have been plotted, a smooth LOESS function can be estimated and its slope (trend) of coefficient of variation would represent the mean variation of Q in time and its temporal turnover.

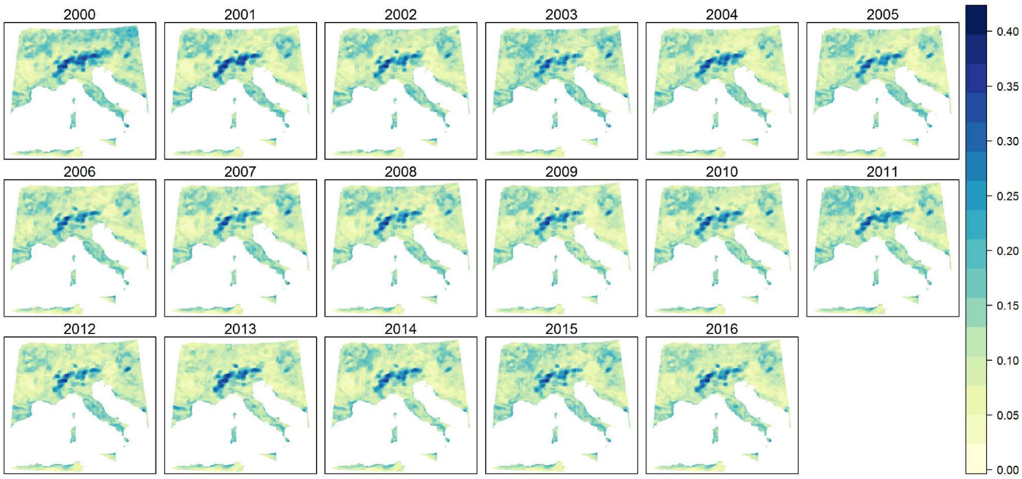

Figure 3: Spatial representation of the free set of Rao's Q data based on MODIS NDVI images at a resolution of 5km provided by Rocchini et al. (2017). The final stack of layers consists of 17 Rao's Q images gathered from 2000 to 2016 in June.

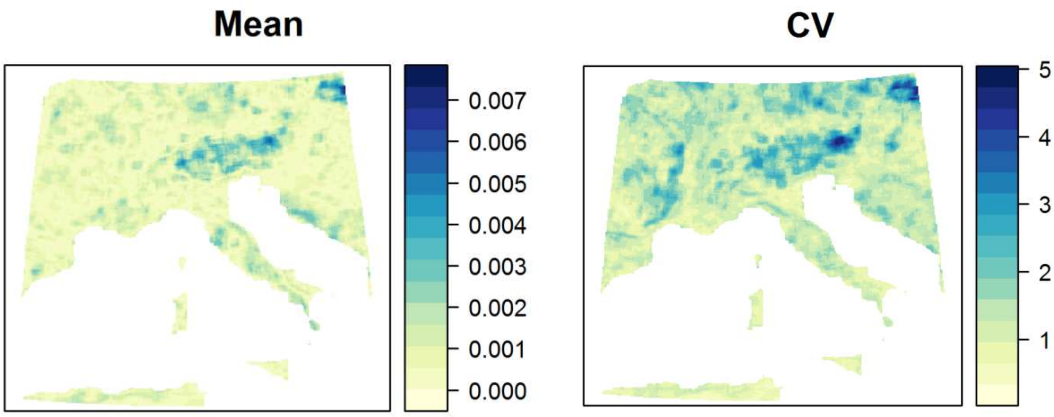

Figure 4: Rao's Q temporal diversity considering LOESS mean slope (mean temporal diversity) and LOESS coefficient of variation (temporal turnover). Both measures detected a higher temporal diversity in areas with higher landscape morphological complexity detected by the spatial Rao's Q.

Appendix 1 - R code

```
########################################
## R CODE FOR APPLYING THE APPROACH PRESENTED IN:
## Rocchini, D., Marcantonio, M., Da Re, D., Chirici, G., Galluzzi, M., Lenoir, J., Ricotta, C., Torresani, M., Ziv, G. (2019). Time-lapsing biodiversity: an open source method for measuring diversity changes by remote sensing. Remote Sensing of Environment.
########################################

## Set working directory and load libraries
setwd("/home/TemporalAlfaDiv/")
library(raster)
library(parallel)
library(fANCOVA) # To automatically select loess smoothing parameters select using aicc
library(ggplot2)
library(rasterVis)
library(plyr)
library(RColorBrewer)
library(gtable)
library(grid)
```

```r
library(gridExtra)
library(ggpubr)

#### 1. Load data ####
load("/home/TemporalAlfaDiv/all_raoQ_5km.RData")
rao_stack<-stack(rao2000_5km, rao2001_5km ,rao2002_5km ,rao2003_5km ,rao2004_5km ,rao2005_5km,
                 rao2006_5km, rao2007_5km, rao2008_5km, rao2009_5km, rao2010_5km, rao2011_5km,
                 rao2012_5km, rao2013_5km, rao2014_5km, rao2015_5km, rao2016_5km)

s<-as.list(rao_stack)

##Cut on Italy
s_red<-mclapply(s, function(x) {y=crop(x,extent(0,20,36,50)); return(y)},mc.cores=detectCores())

##Derive values from raster and put them in a 3D array
rao<-mclapply(s_red,trim,mc.cores=8)
raoV<-mclapply(rao,getValues, mc.cores=8)
raoA<-array(as.numeric(unlist(raoV)), dim=c(336, 275, 17))

#### 2. Apply loess on the time series ####
```

```
#Loess smoothing parameters are automatically selected using aicc
#The derivative of a function is dy/dx, which can be approximated
    by ÎŤy/ÎŤx, that is, "change in y over change in x". This
  can be written in R using diff function
#in order to get an approximation to the derivative of the
  function at each x

stats<-c("mean","min","max")
xl<-seq(2000:2016)
outl <- rep( list(matrix(nrow=336, ncol=275)),3 )
prd <- array( as.numeric(NA), dim=c(336, 275, 17) )

for (r in 1:336) {
  options(warn=-1)
  for (c in 1:275) {
    if(any(is.na(raoA[r,c,]))) {
      next()
    } else {
      prd[r,c,]<-predict(loess.as(seq(1:17), raoA[r,c,],criterion
    = c("aicc"), degree=1, plot = F))
      for (s in 1:3) {
        outl[[s]][r,c]<-sapply(list(diff(prd[r,c,])/diff(xl)),get
  (stats[s]),na.rm=T)
      }
```

```
      }
    }
    options(warn=0)
}

##Make an output raster map
raoTslopes <- stack(s_red[[1]],s_red[[1]],s_red[[1]])

##Add mean, min and max matrices
raoTslopes_out <- stack(lapply(1:3, function(x) {
   values(raoTslopes[[x]])<-as.numeric(outl[[x]]);
   names(raoTslopes[[x]])<-c("mean","min","max")[x];
   return(raoTslopes[[x]])
}))

plot(raoTslopes_out)

## Compute coefficient of variation
rao_stack_it<-crop(rao_stack, extent(0,20,36,50))
rao_stack_it<-stack(rao_stack_it)
rao_mean<-calc(rao_stack_it, mean)
rao_sd<-calc(rao_stack_it, sd)
rao_CV<-((rao_sd)/(1+rao_mean))*100
names(rao_CV)<-"rao_CV"
```

```
raoTslopes_out<-stack(raoTslopes_out, rao_CV)
plot(raoTslopes_out)

##save rasters
stackSave(raoTslopes_out, "raoTslopes")

#### 3. plot ####

##plot parameters
pal<-brewer.pal(9,"YlGnBu")
myTheme <- rasterTheme(region = pal)

utm32n<-" +proj=utm +zone=32 +ellps=WGS84 +datum=WGS84 +units=m +no_defs +towgs84=0,0,0"
crs(raoTslopes_out)<-"+proj=longlat +datum=WGS84 +no_defs +ellps=WGS84 +towgs84=0,0,0"
raoTslopes_out<-projectRaster(raoTslopes_out, crs=utm32n)
p1<-levelplot(abs(raoTslopes_out[[1]]), main= "Mean", scales=list(draw=FALSE), contour = FALSE, margin = FALSE, par.settings = myTheme, ylab= "", xlab= "")
p2<-levelplot(raoTslopes_out[[2]], main= "Min", scales=list(draw=FALSE), contour = FALSE, margin = FALSE, par.settings = myTheme, ylab= "", xlab= "")
```

```
p3<-levelplot(raoTslopes_out[[3]], main= "Max",   scales=list(
    draw=FALSE), contour = FALSE, margin = FALSE,  par.settings =
     myTheme, ylab= "", xlab= "")
p4<-levelplot(abs(raoTslopes_out[[4]]), main= "CV",   scales=list
    (draw=FALSE), contour = FALSE, margin = FALSE,  par.settings
    = myTheme, ylab= "", xlab= "")

grid.arrange(p1,p2,p3,p4, nrow=2)
ggsave("raoRslopes.tiff",  height=8, width=12, units="in", dpi
    =300, plot= pp, path = "/home/TemporalAlfaDiv/img/")

#### Appendix: MODIS NDVI ####
load("/home/TemporalAlfaDiv/all_NDVI_5km.RData")
ndvi_stack<-stack(raster(NDVI_07_2000_5km),raster(NDVI_07_2001_5
    km), raster(NDVI_07_2002_5km), raster(NDVI_07_2003_5km),
                     raster(NDVI_07_2004_5km), raster(NDVI_07_2005_5
    km), raster(NDVI_07_2006_5km), raster(NDVI_07_2007_5km),
                     raster(NDVI_07_2008_5km), raster(NDVI_07_2009_5
    km), raster(NDVI_07_2010_5km), raster(NDVI_07_2011_5km),
    raster(NDVI_07_2012_5km), raster(NDVI_07_2013_5km), raster(
    NDVI_07_2014_5km), raster(NDVI_07_2015_5km),raster(NDVI_07_
    2016_5km))

crs(ndvi_stack)<-"+proj=longlat +datum=WGS84 +no_defs +ellps=
```

```
WGS84 +towgs84=0,0,0"
ndvi_stack<-crop(ndvi_stack, extent(0,20,36,50))
ndvi_stack<-projectRaster(ndvi_stack, crs=utm32n)
annual_ndvi<-as.character(2000:2016)
rastNam<-as.character(2000:2016)

##Time-series plot
mapTheme <- rasterTheme(region=brewer.pal(8,"Greens"))
p12<-levelplot(ndvi_stack,  xlab="", ylab="", scales=list(draw=FALSE),names.attr=rastNam,
                   layout=c(6, 3), contour = FALSE, margin = FALSE,
   par.settings = mapTheme, main= "NDVI 2000-2016")

tiff("img/ndvi2000-2016_GreenTheme.tiff", height = 10, width = 13, res=300,units="in")
p12
dev.off()
```

Appendix 2 - Synthetic example of Rao's Q diversity index calculation

We provide a mathematical example of the calculation of Shannon's H' and Rao's Q diversity indices based on the synthetic examples provided in Figure 1. We will apply such indices to the input image (matrix) I with the highest diversity (Figure 1D). The calculation can then be translated to any matrix.

Let $I = \begin{pmatrix} 1 & 7 & 10 \\ 100 & 102 & 150 \\ 200 & 220 & 255 \end{pmatrix}$ be the input image on which the calculation is applied. Shannon's H' turns out to be $H' = -\sum p \times ln(p)$ where p=proportion of each pixel value. Since p is $\frac{1}{9}$, in this case, hence $H' = 9 \times 0.11 \times ln(0.11) = 2.197$.

Rao's Q diversity adds to such abundance-based calculation the distances among pixel values as $Q = \sum\sum d_{ij} \times p_i \times p_j$. A distance matrix is first calculated, returning $N \times N$ distances, where N=number of input pixels (in this case 9), as:

$$D_i = \begin{pmatrix} 0 & 6 & 9 & 99 & 101 & 149 & 199 & 219 & 254 \\ 6 & 0 & 3 & 93 & 95 & 143 & 193 & 213 & 248 \\ 9 & 3 & 0 & 90 & 92 & 140 & 190 & 210 & 245 \\ 99 & 93 & 90 & 0 & 2 & 50 & 100 & 120 & 155 \\ 101 & 95 & 92 & 2 & 0 & 48 & 98 & 118 & 153 \\ 149 & 143 & 140 & 50 & 48 & 0 & 50 & 70 & 105 \\ 199 & 193 & 190 & 100 & 98 & 50 & 0 & 20 & 55 \\ 219 & 213 & 210 & 120 & 118 & 70 & 20 & 0 & 35 \\ 254 & 248 & 245 & 155 & 153 & 105 & 55 & 35 & 0 \end{pmatrix}.$$

According to the Rao's Q formula, each pairwise distance between the ith and the jth pixel in the image is then multiplied by their proportions p_i and p_j, hence by $\frac{1}{9} \times \frac{1}{9} = \frac{1}{81} = 0.0123$.

Extracting all these terms and applying the sum as in Equation 1 will lead to a final value of $Q = 102.963$, as in Figure 1D.

In the additional Supplementary Material we also provide a spreadsheet with the calculation of Shannon's H' and Rao's Q indices for the four environmental situations reported in Figure 1.

Appendix 3 - Sketch of the original NDVI values used to calculate Rao's Q

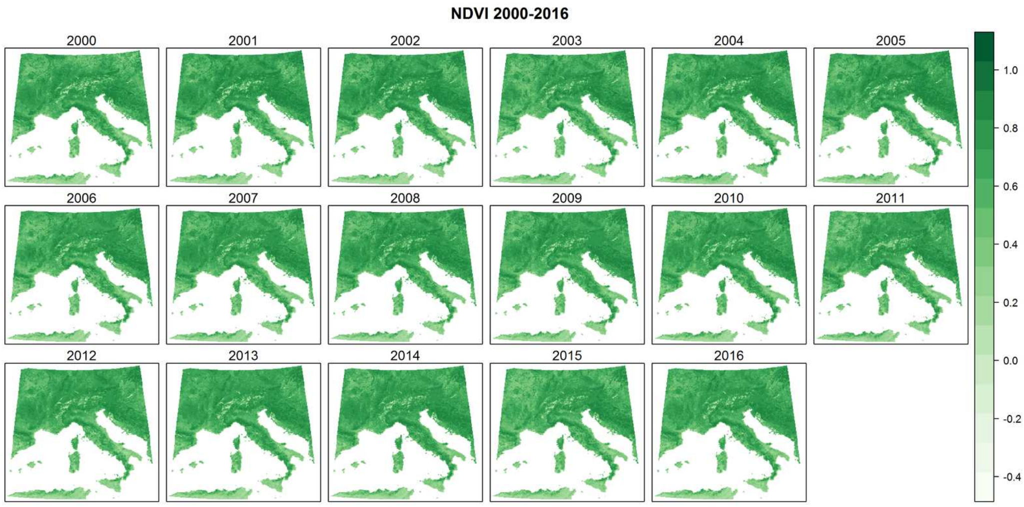

This graph represents the sketch of NDVI maps from which the Rao's Q diversity has been derived and provided for free by Rocchini et al. (2018).